

Supporting information

Influence of Na⁺ ion doping on the phase change and upconversion emissions of the GdF₃: Yb³⁺, Tm³⁺ nanocrystals obtained from the designed molecular precursors

**Hana Ayadi,^a Wenzhang Fang,^{a,b} Shashank Mishra,^{*a} Erwann Jeanneau,^c Gilles
Ledoux,^d Jinlong Zhang^b and Stéphane Daniele^a**

^a Université Lyon 1, CNRS, UMR 5256, IRCELYON, Institut de recherches sur la catalyse et l'environnement de Lyon, 2 avenue Albert Einstein, F-69626 Villeurbanne, France

^b Key Laboratory for Advanced Materials and Institute of Fine Chemicals, East China University of Science and Technology, 130 Meilong Road, Shanghai 200237, China

^c University of Lyon1, Centre de Diffractométrie Henri Longchambon, 5 rue de La Doua, 69100 Villeurbanne, France

^d University of Lyon1, Institut Lumière Matière, UMR5306 CNRS, Bâtiment Kastler, 10 rue Ada Byron, 69622 Villeurbanne, France

E-mail: shashank.mishra@ircelyon.univ-lyon1.fr; Fax: 33-472445399; Tel: 33 472445322.

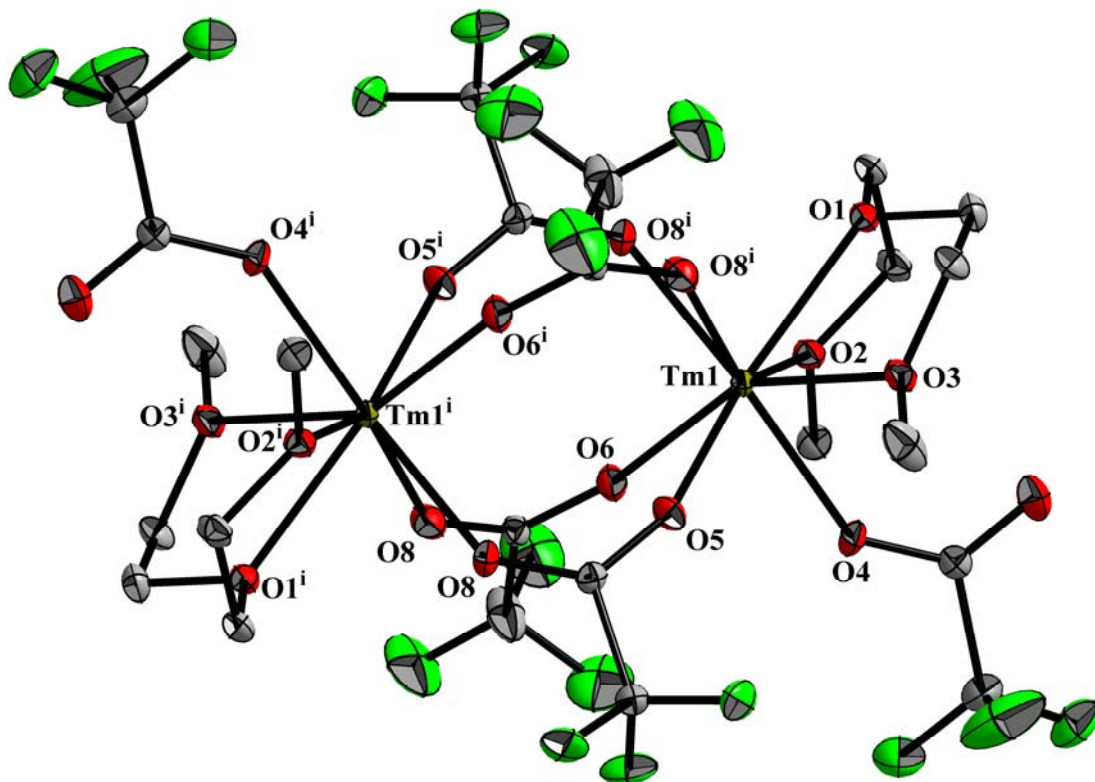


Fig. S1 Perspective view of $[\text{Tm}_2(\text{TFA})_6(\text{diglyme})_2]$ (**2**). H-atoms on diglyme ligand have been omitted for clarity. Selected bond lengths (\AA) and angles ($^\circ$): Tm1—O9 2.434 (5), Tm1—O27ⁱ 2.315 (5), Tm1—O11 2.267 (4), Tm1—O13ⁱ 2.310 (5), Tm1—O18 2.236 (4), Tm1—O2 2.383 (4), Tm1—O25 2.260 (5), Tm1—O5 2.439 (5), O27ⁱ—Tm1—O13ⁱ 72.42 (18), O2—Tm1—O18 106.92 (16), O2—Tm1—O5 67.24 (15), O5—Tm1—O18 76.11 (17), O2—Tm1—O9 66.05 (16), O9—Tm1—O18 74.04 (17), O5—Tm1—O9 112.43 (16), O2—Tm1—O18 106.92 (16), O2—Tm1—O11 144.56 (17), O2—Tm1—O25 138.44 (17), O5—Tm1—O11 144.74 (16), O5—Tm1—O25 76.50 (16), O9—Tm1—O11 82.62 (17), O9—Tm1—O25 151.28 (17), O11—Tm1—O25 76.59 (18), O11—Tm1—O18 78.12 (17). Symmetry code: (i) $-x, -y+1, -z+1$

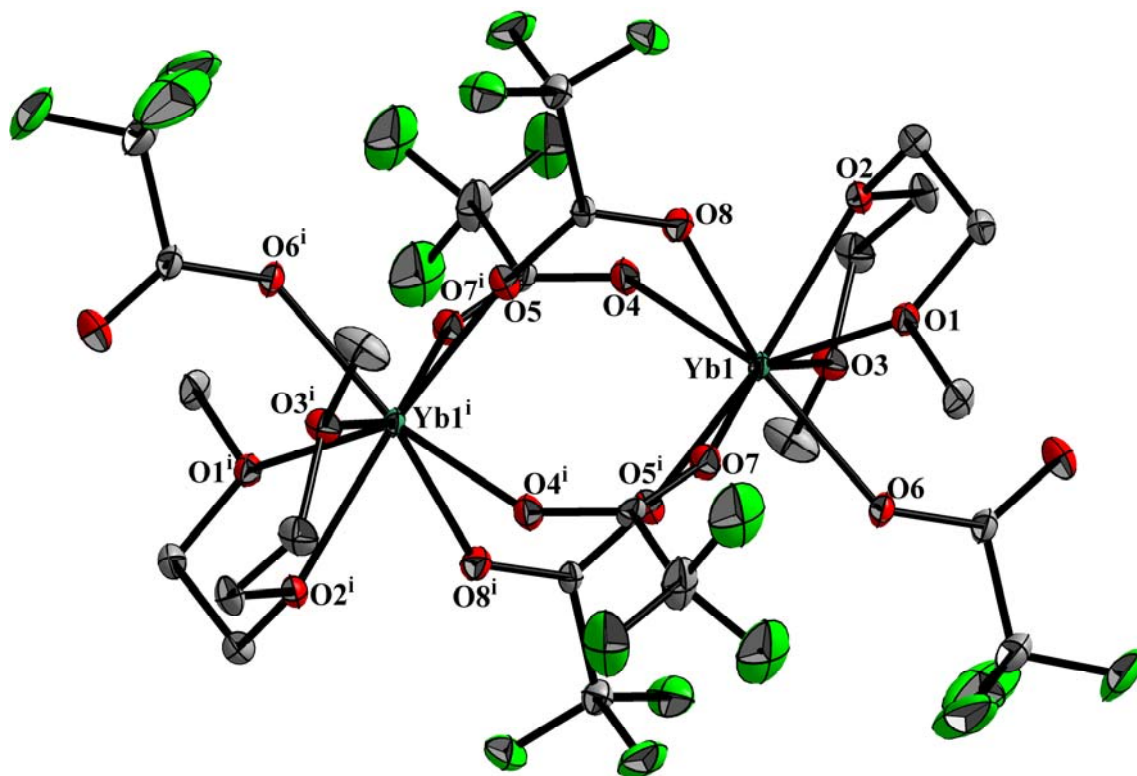


Fig. S2 Perspective view of $[\text{Yb}_2(\text{TFA})_6(\text{diglyme})_2]$ (**3**). H-atoms on diglyme ligand have been omitted for clarity. Selected bond lengths (\AA) and angles ($^\circ$): Yb1—O4^i 2.307 (5), Yb1—O25 2.430 (4), $\text{Yb1}^i\text{—O11}^i$ 2.258 (5), Yb1—O28 2.226 (4), Yb1—O19 2.430 (5), $\text{O4}^i\text{—Yb1}^i\text{—O11}^i$ 77.56 (17), O2—Yb1—O22 144.44 (17), O2—Yb1—O9 74.69 (18), O9—Yb1—O22 79.63 (16), $\text{O4}^i\text{—Yb1—O19}$ 76.08 (17), O2—Yb1—O25 82.68 (17), $\text{O11}^i\text{—Yb1—O19}$ 76.33 (17), O9—Yb1—O25 71.95 (17), O2—Yb1—O19 144.79 (17), O2—Yb1—O28 78.06 (18), O9—Yb1—O19 139.38 (17), O9—Yb1—O28 138.48 (18). Symmetry code: (i) $-x, -y+1, -z+2$.

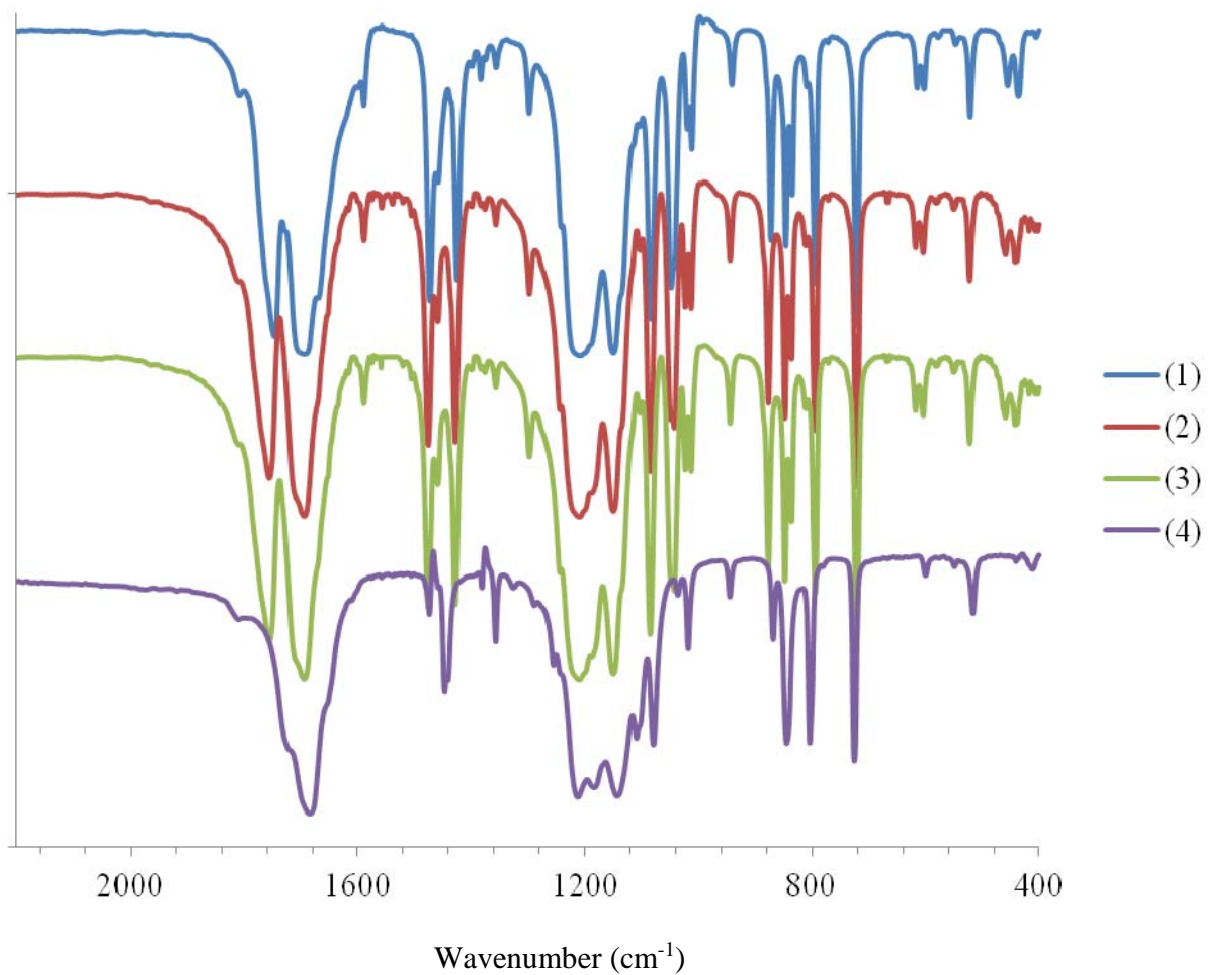


Fig. S3 FT-IR spectra of (1)-(4) measured as nujol mulls.

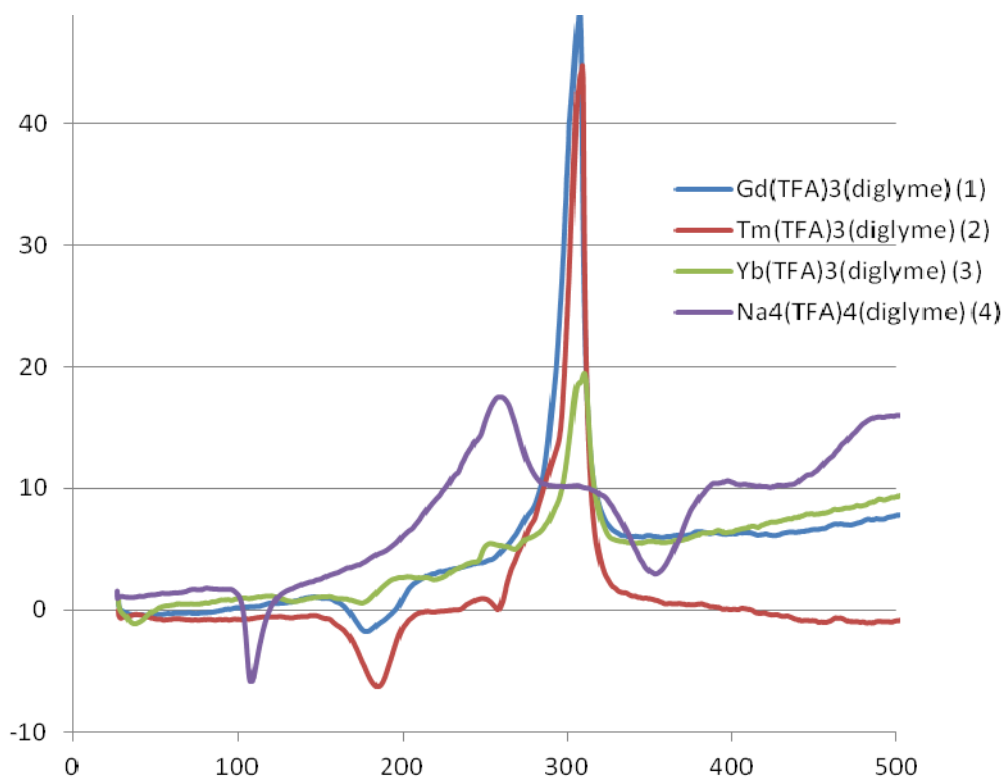


Fig. S4 DTA curves of **1-4**.

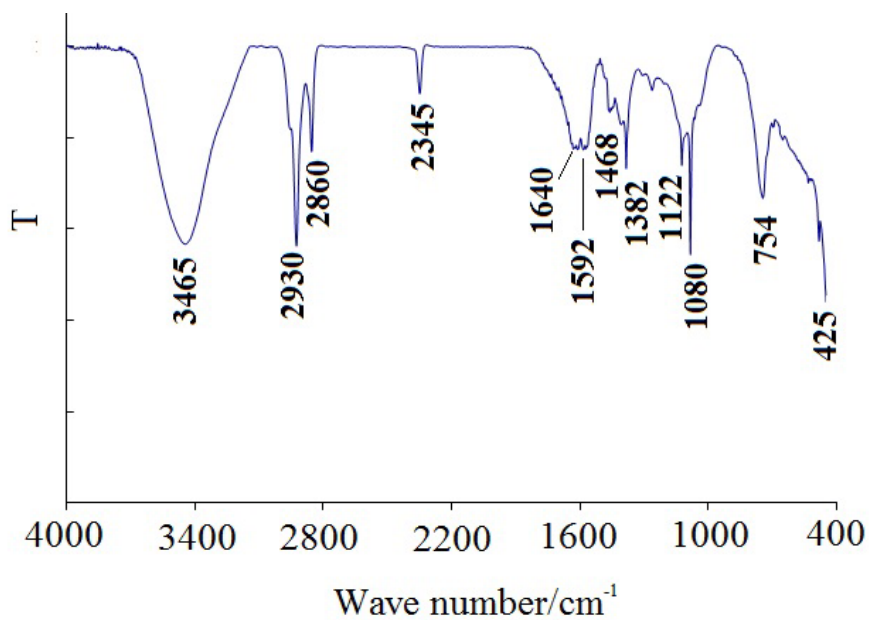


Fig. S5 IR spectrum of as-prepared $\text{GdF}_3:\text{Yb}^{3+}, \text{Tm}^{3+}$ NCs.

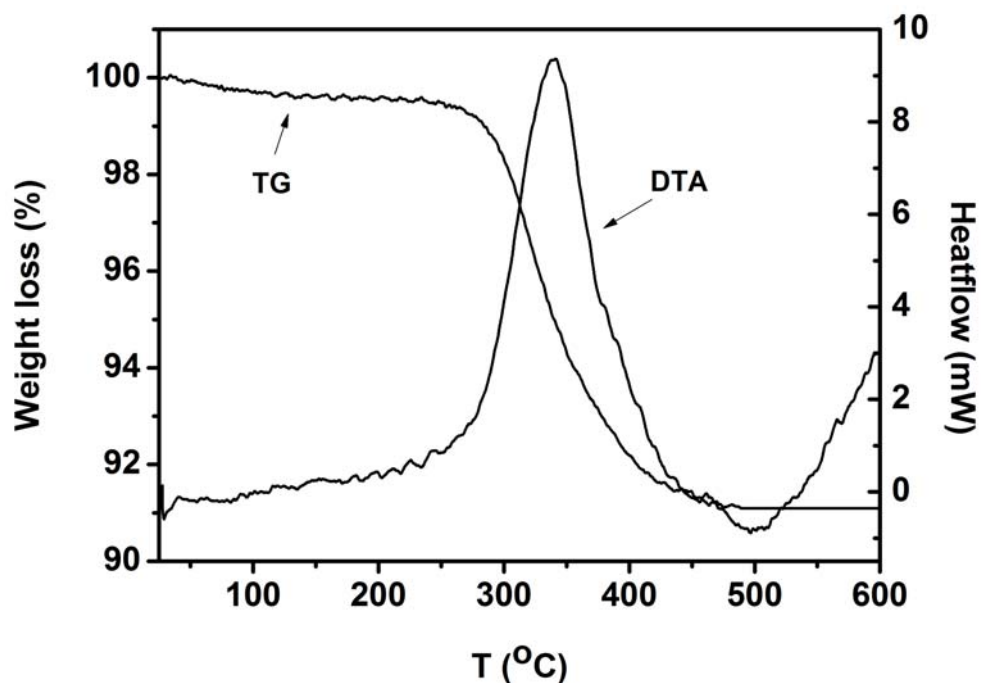


Fig. S6 TG-DTA curves of as-prepared $\text{GdF}_3:\text{Yb}^{3+}, \text{Tm}^{3+}$ NCs.

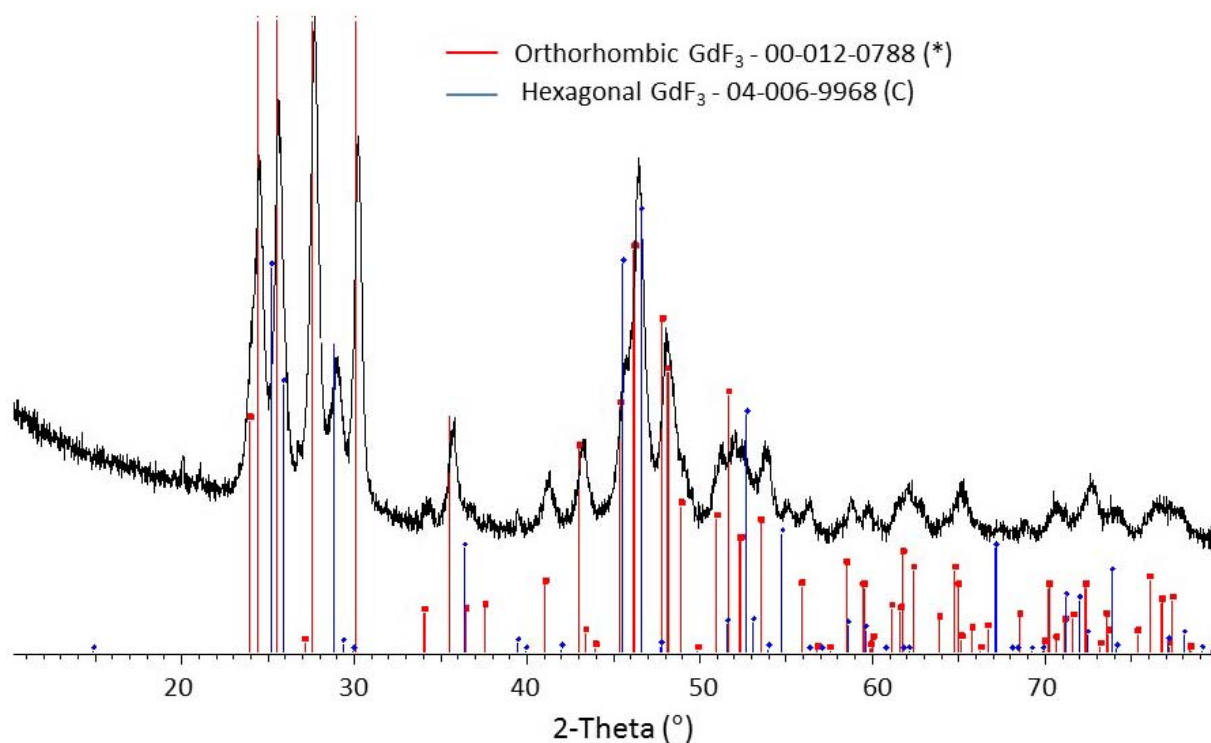


Fig. S7 XRD of $\text{GdF}_3: 20\% \text{Yb}^{3+}, 2\% \text{Tm}^{3+}, 20 \text{ mol}\% \text{Na}^+$ NCs.

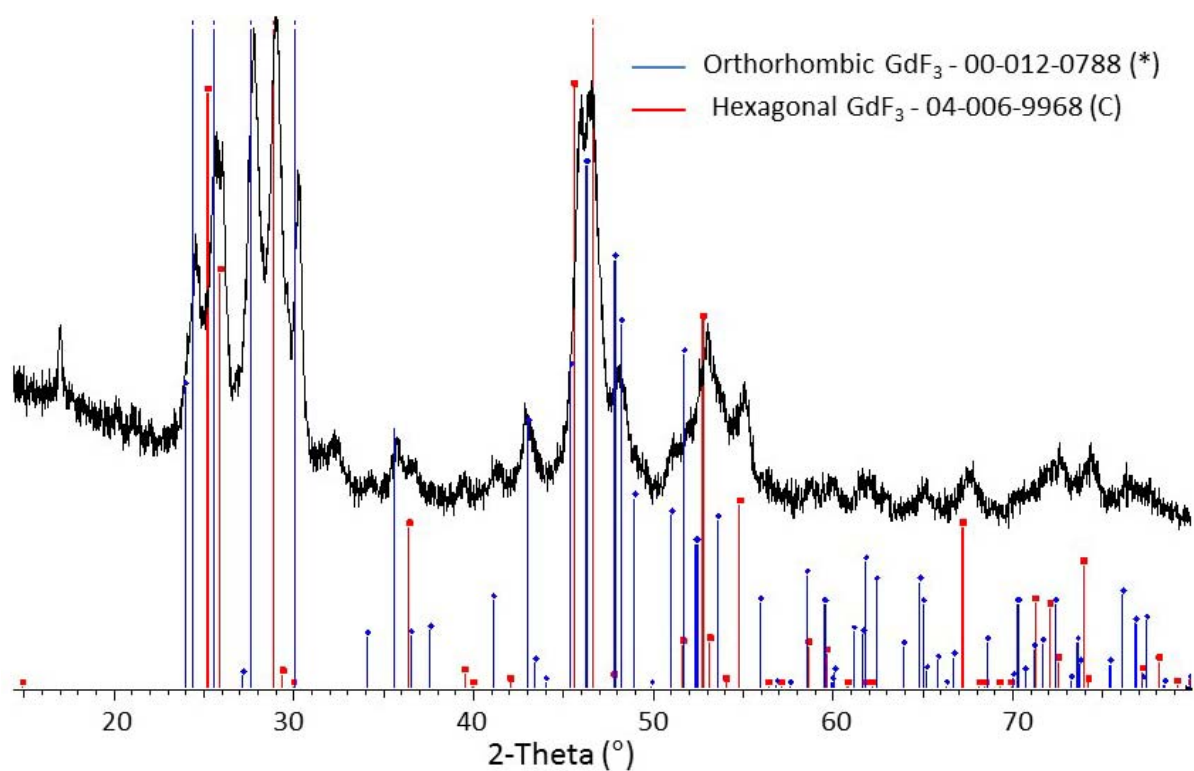


Fig. S8 XRD of GdF_3 : 20% Yb^{3+} , 2% Tm^{3+} , 30 mol% Na^+ NCs.

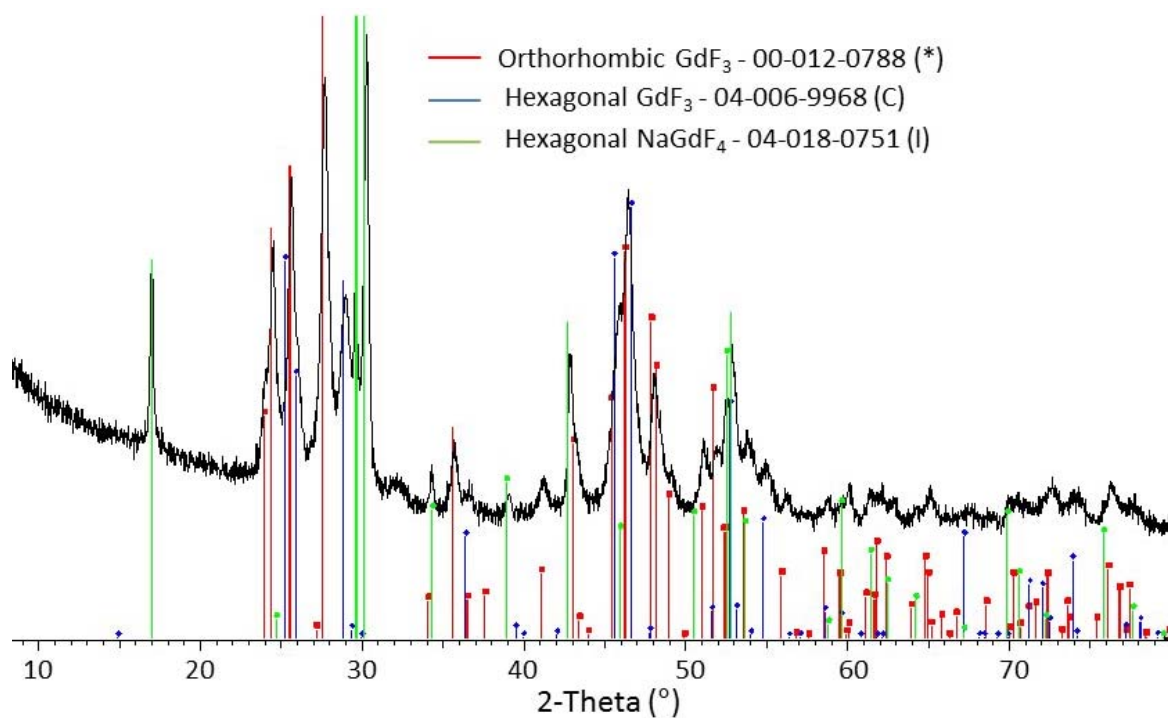


Fig. S9 XRD of GdF_3 : 20% Yb^{3+} , 2% Tm^{3+} , 40 mol% Na^+ NCs.

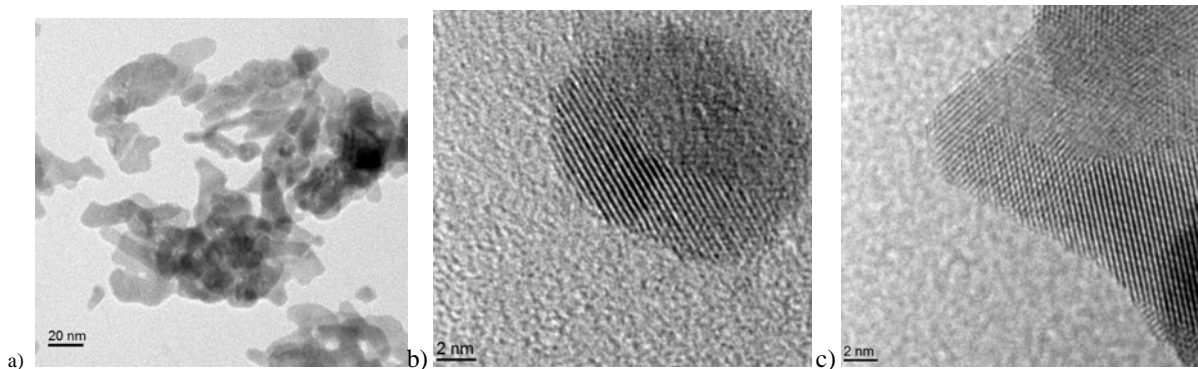


Fig. S10 TEM and HR-TEM images of as-prepared $\text{GdF}_3:\text{Yb}^{3+}, \text{Tm}^{3+}$ NCs.

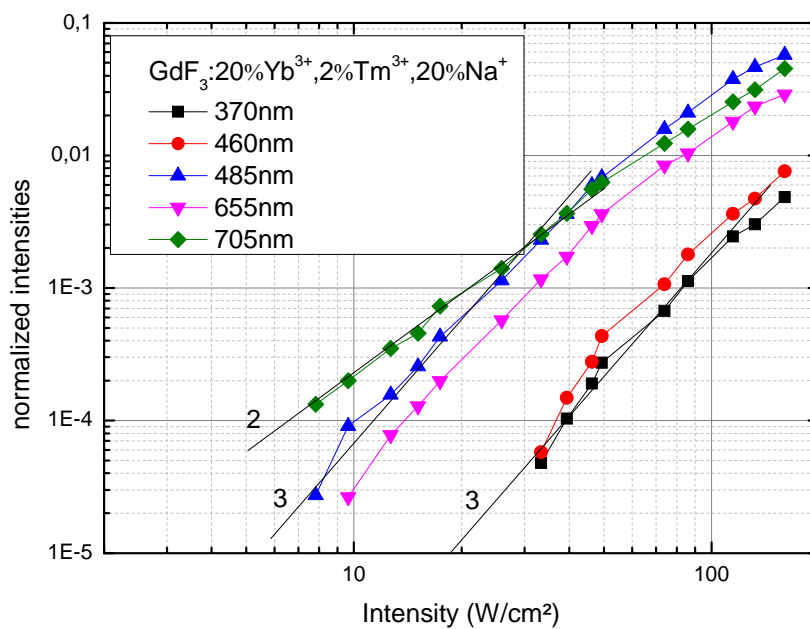


Fig. S11 Evolution of the intensity of the different bands of $\text{GdF}_3: 20\% \text{Yb}^{3+}, 2\% \text{Tm}^{3+}, 20\% \text{Na}^+$ NCs with the fluence.

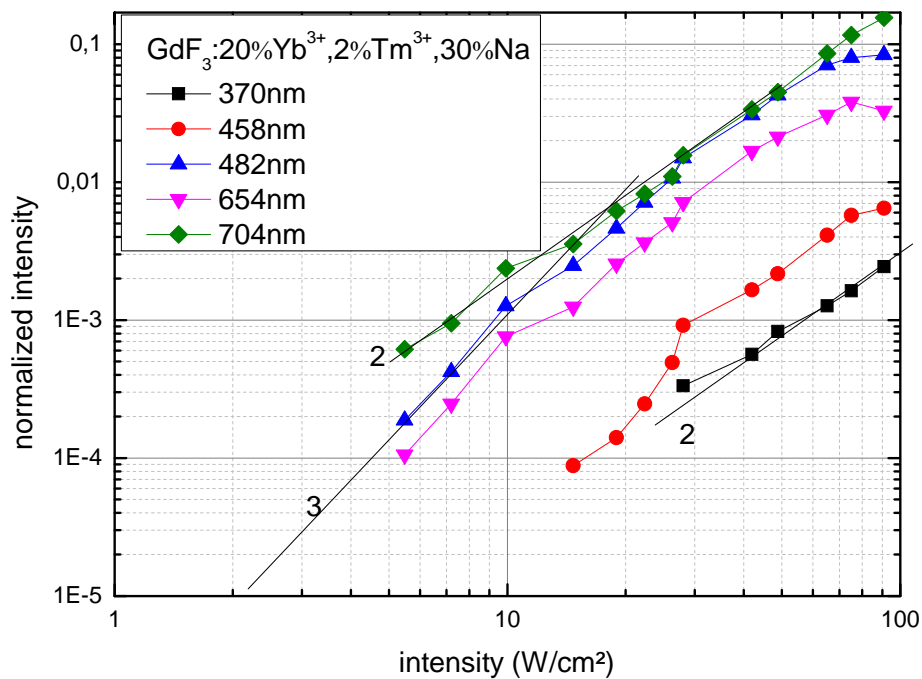


Fig. S12 Evolution of the intensity of the different bands of $\text{GdF}_3: 20\% \text{Yb}^{3+}, 2\% \text{Tm}^{3+}, 30\% \text{Na}^+$ NCs with the fluence.

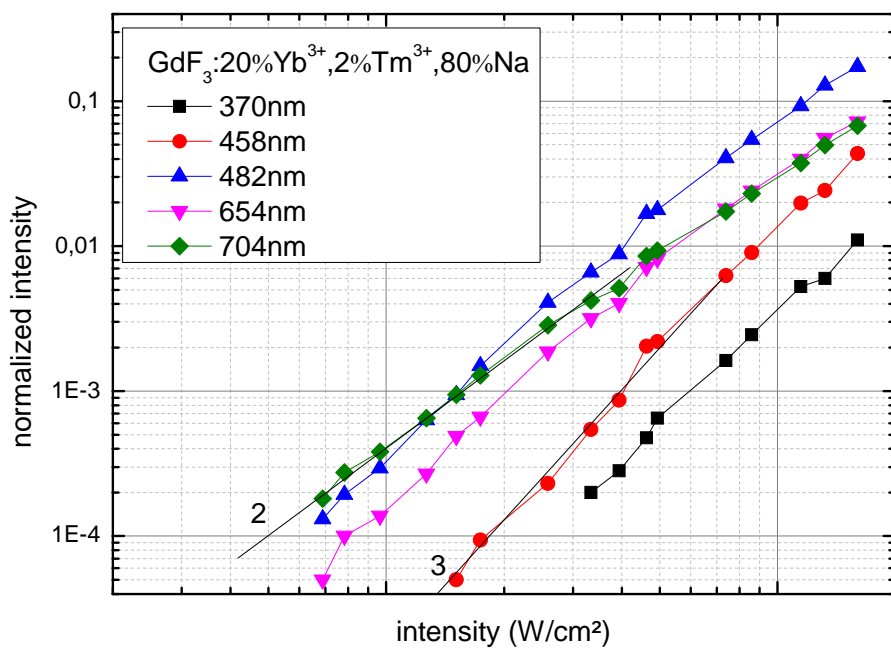


Fig. S13 Evolution of the intensity of the different bands of $\text{GdF}_3: 20\% \text{Yb}^{3+}, 2\% \text{Tm}^{3+}, 80\% \text{Na}^+$ NCs with the fluence.

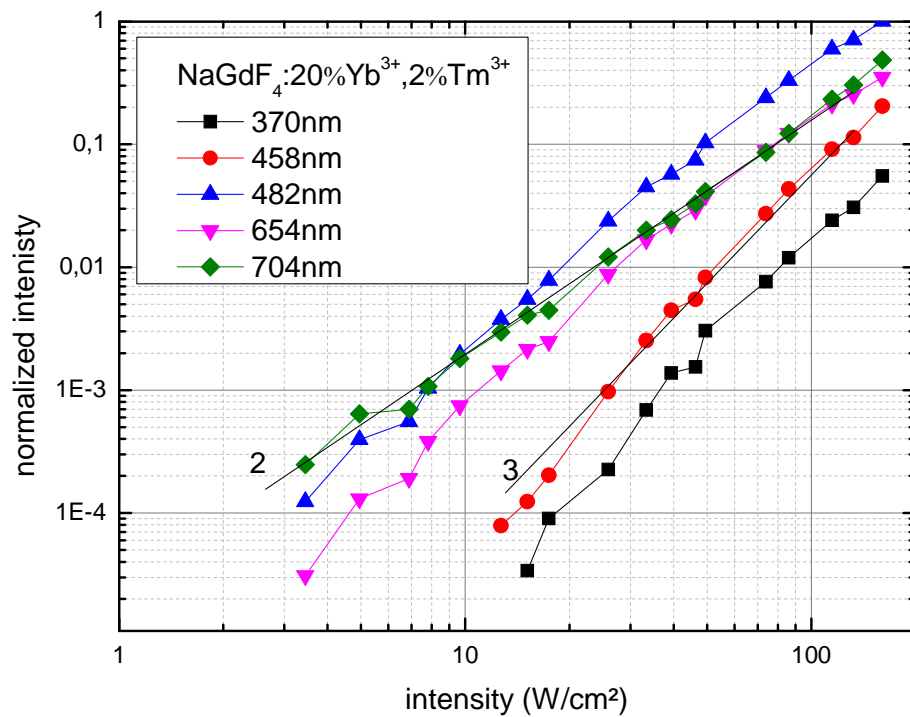


Fig. S14 Evolution of the intensity of the different bands of NaGdF₄: 20% Yb³⁺, 2% Tm³⁺ NCs with the fluence.